JOURNAL OF MATERIALS SCIENCE 21 (1986) 1005–1010

Fracture mechanism of unidirectional carbon-fibre reinforced epoxy resin composite

NORIO SATO, TOSHIO KURAUCHI, OSAMI KAMIGAITO
Toyota Central Research and Development Laboratories, Inc, Nagakute-cho, Aichi-gun, Aichi-ken, 480-11, Japan

The object of this study was to investigate the fracture mechanism of unidirectional carbon-fibre reinforced epoxy resin composite. For this purpose, the failure process of the composite under load was observed *in situ* by scanning electron microscopy and the matrix deformation around the broken fibre tip was examined by polarized transmission optical microscopy using a thin section of the composite. The failure process was shown to proceed through the following four stages: (1) fibre breakage began to occur at a load of about 60% of the failure load; (2) as the applied load was increased, plastic deformation occurred first from the broken fibre tip along the fibre sides, followed by final matrix cracking in the plastic region; (3) just before failure, partial delamination occurred, originating from fibre breakage and matrix cracking; (4) finally, a catastrophic crack propagation occurred from the delamination, leading to composite failure. Acoustic emission monitoring was also carried out for non-destructive evaluation, which indicated that internal failure began to occur at a load of 60% of the failure load and propagated remarkably before composite failure. A close correspondence between the acoustic signal and crack formation was obtained. The acoustic signal at lower amplitude, occurring over whole load range, corresponded to fibre breakage and matrix cracking while that at higher amplitude, occurring only just before failure, corresponded to partial delamination. From these experimental studies, the fracture mechanism of the composite has been clarified.

1. Introduction

Fibre-reinforced plastic composites have been used in various fields of industry. In the automobile industry, applications of these composites to such structural components as drive shafts and leaf springs are undertaken. For assurance of the reliability of these structural products, a study of their failure mechanism is very important. In addition, the study may be useful also in the selection of fibres and matrix materials and the optimum design of structural products.

Many studies on composite failure have been made. However, most are concerned with macroscopic failure behaviour or failure mode. Relatively few studies have been made on the failure mechanism of composites. For example, Zweben and Rosen [1, 2] analysed the instability of an initial crack originating from broken fibres and proposed an approximation of a failure load. Harlow and Phoenix [3] made a probabilistic approach to the occurrence of fibre breakage resulting from the stress concentration around broken fibre tips. Mahishi and Adams [4] analysed the fracture behaviour of a single-fibre model composite by an elastoplastic finite element method and predicted the process of initiation and propagation of the crack. White and Tretout [5] used acoustic emission (AE) monitoring to study the failure mechanism of a single-fibre model composite by applying frequency analysis. On the other hand, Becht *et al.* [6] applied AE amplitude distribution analysis to distinguish different failure modes in various fibre-reinforced composites. These studies have clarified the overall mechanism of failure to some extent; however, detailed mechanism has been left unclarified due to lack of experimental study of the fracture process in practical composites.

In the present work, experimental studies have been undertaken to investigate the fracture mechanism of unidirectional carbon-fibre reinforced epoxy resin composite. For this purpose, the detailed failure process of the composite under load was observed *in situ* by scanning electron microscopy (SEM), as proposed in our previous studies [7, 8]. A thin section of the composite was also examined by polarized optical microscopy to observe plastic deformation of the matrix around the broken fibre tips. Furthermore, the acoustic emission technique was used to detect the failure process for a non-destructive evaluation.

2. Experimental procedure

2.1. Composite specimen

Unidirectional carbon-fibre reinforced epoxy resin composite was used for this study. The composite plate was made of prepreg consisting of carbon fibre (Pyrofil, high-strength type) and epoxy resin (Epikote 210 cured with accelerator $BF_3 \cdot MEA$), which was purchased from Mitsubishi Rayon Co, Ltd, Japan. The prepreg was laminated unidirectionally to thicknesses of 1 and 3 mm, and cured in a hot press at 170° C for 1 h. The composite obtained was post-cured

0022–2461/86 $03.00 + .12

TABLE I Mechanical properties of carbon fibre, epoxy resin and unidirectional carbon-fibre reinforced epoxy resin composite

Fibre (High-strength carbon fibre)	
Diameter of fibre (μm)	8
Tensile strength (GPa)	2.9
Young's modulus (GPa)	245
Matrix (Epikote 210 and BF_3MEA)	
Tensile strength (MPa)	68
Fracture strain (%)	3
Young's modulus (GPa)	2.9
Composite (Fibre direction)	
Volume fraction of fibre (%)	60
Bending strength (GPa)	1.76
Bending modulus (GPa)	113

at 170° C for 3 h in an air-circulating oven. Two types of specimens was prepared by cutting the composite plates with a diamond-impregnated tool. One was 170 mm long, 20 mm wide and 3 mm thick for acoustic emission tests, and the other was 60 mm long, 10 mm wide and 1 mm thick for SEM and optical microscopic observations. The mechanical properties of the carbon fibre, epoxy resin and composite are listed in Table I.

2.2. Acoustic emission monitoring

AE monitoring was carried out at a three-point bending test by use of the system, Dunegan/Endevco 3000 series. The test conditions are shown in Fig. 1. The piezoelectric transducer (resonant peak at 140 kHz) was attached to the specimen using an adhesive tape clamp. The specimen was subjected to a bending load with the crosshead speed of 5 mm min^{-1}. The AE signal detected by the transducer was submitted to highpass-filter (100 kHz) and amplified with a preamplifier and a main amplifer. The total system amplification was maintained at 87 dB. A cumulative AE event count was obtained with a pulse analyser which was adjusted to count only the AE signals which exceeded a threshold value (1 V). Simultaneously, each AE signal amplified with a preamplifier (40 dB) was sorted with a distribution analyser according to its maximum value of amplitude. This data analysis showed maximum amplitude distribution of AE signals, which was a spectrum of population of AE events against their maximum amplitude. The cumulative AE event count and maximum amplitude distribution were recorded as a function of applied bending load. The cumulative AE event count data were used to analyse the crack initiation and propagation of the composite and the amplitude distribution data were used to distinguish between different crack origins [8].

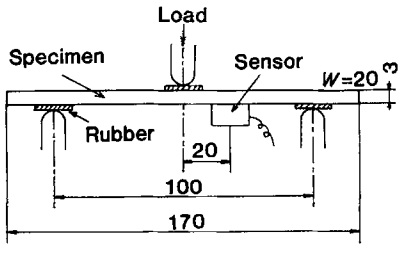

Figure 1 Three-point bending test and AE monitoring apparatus, *W*; specimen width (mm).

2.3. *In situ* SEM observation

The surface of the specimen under load was examined by SEM in order to observe the detailed failure process of the specimen directly. For this purpose, the specimen was bent by a small three-point bending device and held under load. The specimen under load was coated with gold by a PVD technique and set up in the SEM apparatus. The tensile surface of the specimen near maximum deflection was examined by SEM. After examination, the specimen was further bent slightly and coated again, and the SEM examination was again carried out. The same procedure was repeated until the specimen failed. Therefore, the detailed failure process of the specimen could be observed *in situ* (*in situ* SEM observation).

2.4. Polarized transmission optical microscopic observation

A thinned section of the specimen was examined by polarized transmission optical microscopy in order to study the deformation of the matrix around the broken fibre. At first, the specimen was subjected to a three-point bending test to induce fibre breakage on the tensile surface, and the bending load was removed. The specimen was polished on the compressive side using standard metallographic polishing techniques. Polishing was completed, to make the specimen a single layer of fibre and matrix (approximately 10 μm). The thinned section was thin enough to transmit light through the matrix region. Therefore, the state of matrix deformation around the broken fibre could be examined by birefringence.

3. Results

3.1. AE monitoring

Fig. 2 shows the load–deflection curve and cumulative AE event count obtained by a three-point bending test. The specimen was elastically deformed to maximum load and failed in a brittle manner. AE signals began to occur at a load of about 60% of the failure load and remarkably increased in a load range higher than 80% of the failure load. This result indicated that internal failure began to occur gradually at a relatively low load and propagated rapidly near the maximum

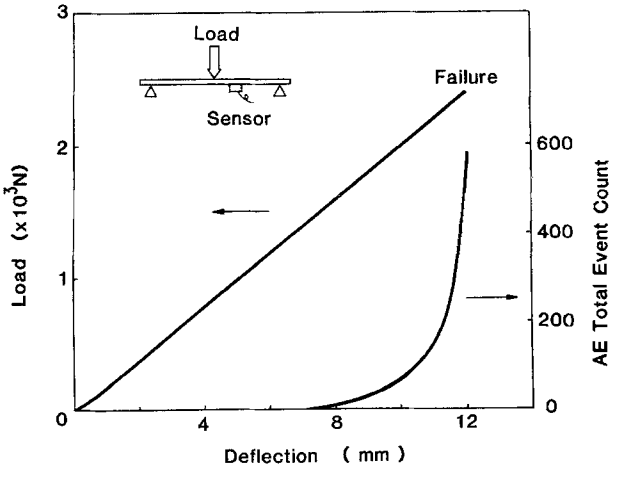

Figure 2 Load–deflection curve of the composite in the three-point bending test and the cumulative AE event count.

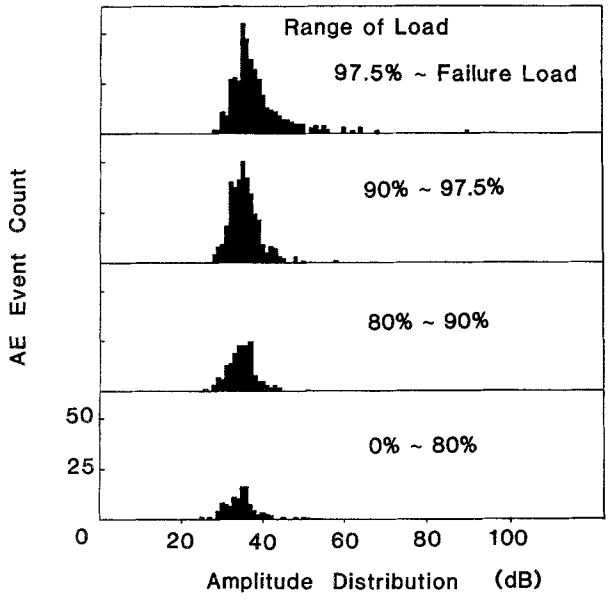

Figure 3 Amplitude distribution analysis of the AE signal for various load ranges up to composite failure.

load, although the load–deflection curve showed a linear elastic behaviour until the final failure.

Fig. 3 shows the result of maximum amplitude distribution of the AE signal obtained for various load ranges up to failure. In the spectra, the population curves could be separated into two parts according to the amplitude value. One was a sharp population curve with a mean amplitude of 35 dB observed in all load ranges. The other was a broad population curve with an amplitude ranging from 40 to 90 dB, observed in only the final load range. The value of amplitude of the AE signal is considered to correspond to the value of elastic energy released by the formation of a crack. An AE signal of lower amplitude is attributed to crack formation which releases a small elastic energy, and an AE signal of higher amplitude is originated from the crack which releases relatively large elastic energy. Therefore, the amplitude distribution obtained in this study was considered to indicate the occurrence of two different types of cracks in the failure process of the composite.

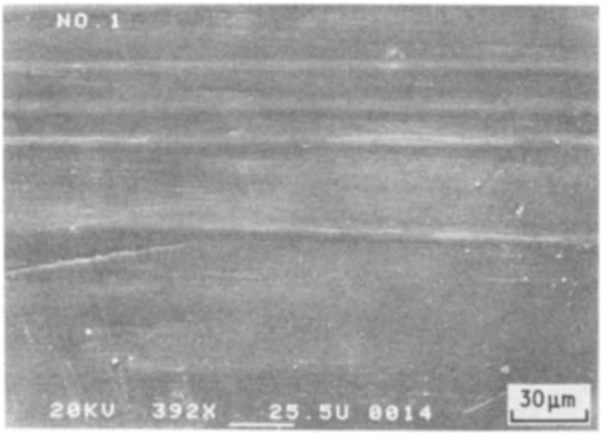

Figure 4 As-cured surface of the specimen. Lateral lines indicate the presence of a fibre beneath the surface.

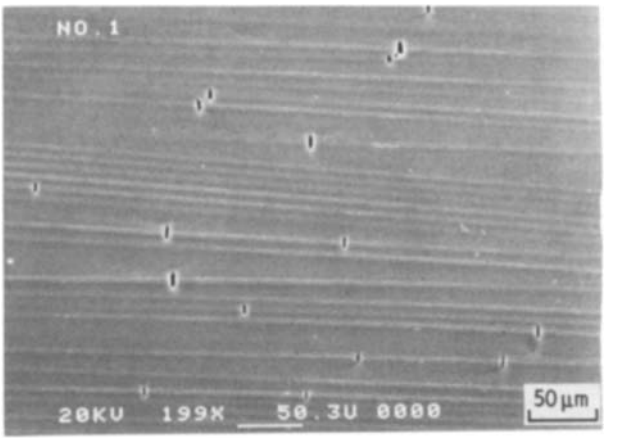

Figure 5 Fibre breakage, first indication of failure, observed under a stress of about 70% of the failure stress.

3.2. *In situ* SEM observation of failure process

The failure processes obtained by *in situ* SEM observation are shown in Figs 4 to 11. Fig. 4 shows an as-cured surface of the specimen in the initial stage. The surface was slightly uneven due to the presence of fibres beneath the surface. The lateral lines indicate the presence of each fibre embedded in the matrix, thus it was possible to distinguish each fibre from the matrix. Initial damage caused by the cure process was barely observed in the matrix, fibre or interface. The specimen was loaded along the fibre direction by a three-point bending device. As the first indication of failure, a fibre was broken under a relatively low load. Figs 5 and 6 show fibre breakages observed under a stress of about 70% of the failure stress of specimen. Fibre breakage occurred randomly and the crack did not propagate into the matrix in this stress stage. The occurrence of fibre breakage was considered to be the first indication of composite failure.

As the stress was increased further, many fibres broke. At the same time, a matrix crack was generated, starting from a broken fibre tip. A typical example of matrix cracking is shown in Fig. 7, which was observed under a stress of about 90% of the failure stress of specimen. The matrix crack occurred from the broken fibre tip and propagated along the side of the fibre. Then, the crack was considered to be

Figure 6 A magnified view of the fibre breakage.

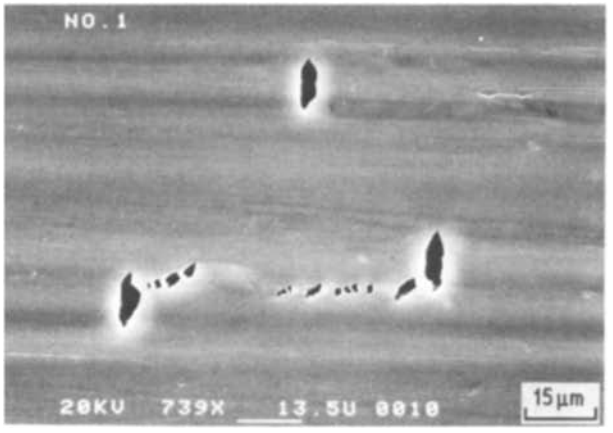

Figure 7 Matrix crack, second indication of failure, observed under a stress of about 90% of the failure stress.

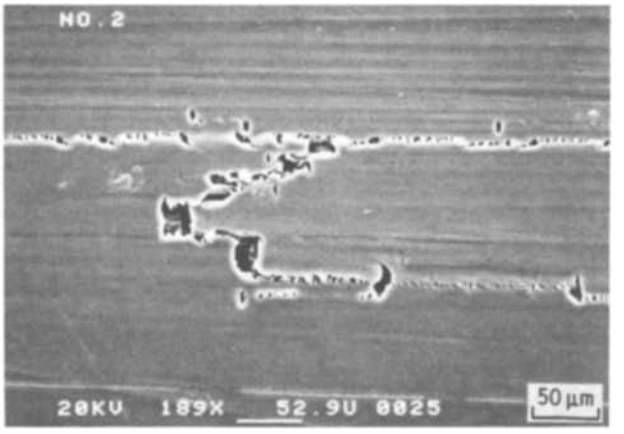

Figure 9 Partial delamination, third indication of failure, observed under a stress nearly equal to the failure stress.

formed due to the shear stress concentration generated by the fibre breakage. Fig. 8 shows the growth of a matrix crack obtained with a slight increment of the applied stress. The initiation and growth of the matrix crack accompanied by fibre breakage was considered to be the second indication of composite failure.

As the stress was further increased, approximately to the failure stress, fibre breakage and matrix cracking were increased and a partial delamination occurred abruptly starting from the fibre breakage and matrix crack. Fig. 9 shows a typical example of partial delamination observed under a stress nearly equal to the failure stress. Fibre breakage and matrix cracking were responsible for the occurrence of delamination. Judging from the geometry of delamination, more than ten fibres were broken and a large matrix crack was spread under the delamination. Just before failure, some partial delaminations occurred and they grew together. Fig. 10 shows the growth of partial delamination observed just before failure. The occurrence and growth of partial delamination was considered to be the third indication of composite failure.

When the partial delamination grew to some size, a catastrophic crack propagation occurred through the specimen, leading to the final failure. Fig. 11 shows the fracture surface indicating a brittle failure mode of the specimen. This fast crack propagation was the final indication of composite failure.

3.3. Microscopic observation of matrix deformation

Fig. 12 shows polarized optical micrographs of a thinned section of the specimen. Brightened and darkened regions in the matrix are considered to indicate the plastic deformation of the matrix. Figs 12a and b show the plastic deformation propagating from broken fibre tips along the fibre sides. Fig. 12c indicates the plastic zone connecting neighbouring fibre tips. The plastic deformation was considered to be generated by the shear stress due to the fibre breakage. The deformation was observed to propagate along the fibre sides, but not to expand to the next matrix region across fibres. Expansion of the plastic deformation was observed to be suppressed by the presence of neighbouring fibres.

4. Discussion

The failure process of the composite observed by *in situ* SEM observation was studied in terms of the microscopic stress state. In the early stage of the composite deformation, fibre and matrix were deformed uniformly. They were considered to be under equal strain states. When the fibre stress reached some value, a fibre was broken as the first indication of failure. The breakage was considered to be caused by a defect in

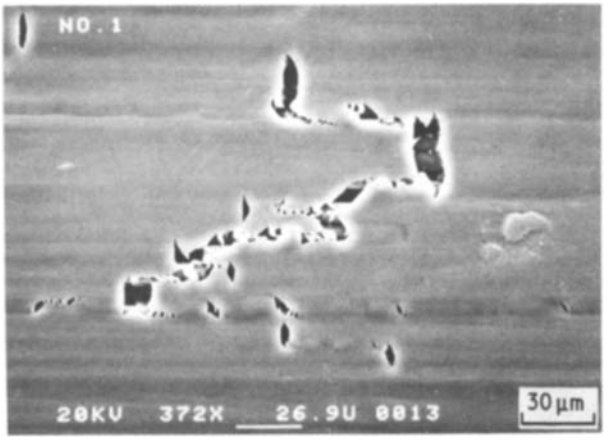

Figure 8 Fibre breakage and matrix crack observed under a stress of about 90% of the failure stress.

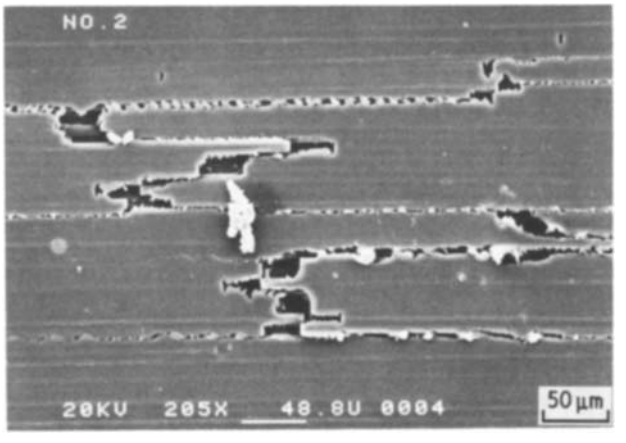

Figure 10 Partial delamination observed just before failure.

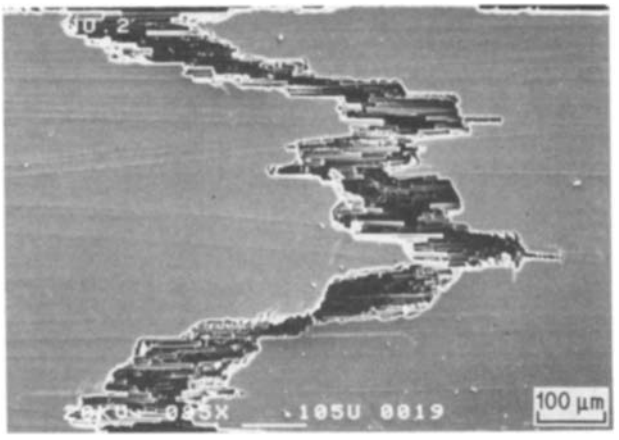

Figure 11 Fracture surface, final indication of failure, observed after failure.

the fibre because it occurred randomly at a relatively low load. The uniform deformation of the matrix was disturbed by the occurrence of fibre breakage. The shear stress was concentrated in the vicinity of the broken fibre tip and in the region along the fibre sides. Then, the matrix around the fibre tip was deformed extremely by the shear stress concentration, and the matrix crack was formed starting from the fibre tip. As the applied load was further increased approximately to the failure load, fibre breakage and matrix cracking occurred frequently. In such a high stress stage, fibres were broken by the stress concentration caused by adjacent broken fibre tips, thus fibre breakage was concentrated in a localized region. These fibre breakage and matrix cracks were responsible for the occurrence of partial delamination. Just before failure, a few partial delaminations occurred and they grew together to some size. Finally, catastrophic crack propagation occurred from the partial delamination, leading to composite failure.

Correlation between the AE signal and crack formaformation was analysed by comparing the AE data with results of SEM observations in the same load range. Fig. 2 shows that the AE signal began to occur at the load range of about 60% to 80% of the failure load. In the same load range, random fibre breakage was observed by *in situ* SEM observation as the first indication of failure. Therefore, the initial occurrence of the AE signal was considered to correspond to the fibre breakage. Similarly, the AE signal occurring in a load range of about 80% to 90% of the failure load could be related to the formation of fibre breakage and matrix cracking. A remarkable increment of AE signal just before failure could be related to the formations of fibre breakage, matrix cracking and partial delamination.

As the load was increased, however, it was difficult to correlate each AE signal clearly to each crack formation. In order to obtain more clear correlation, the AE signal was analysed according to the maximum amplitude distribution. The value of the maximum amplitude of the AE signal was considered to correspond to that of the elastic energy released by the formation of a crack. In Fig. 3, the AE signal of lower amplitude was considered to be emitted from the crack which released a small elastic energy, and the AE signal of higher amplitude was considered to be emitted from the crack which released a larger elastic energy. Judging from the geometry of cracks observed by SEM, fibre breakage and matrix cracking were considered to release only small elastic energy, because the fibres were very fine and the modulus of the matrix was very low. On the other hand, partial delamination was considered to release an extremely large elastic energy, because it consisted of many fibre breakages and a large matrix crack between laminates. Therefore, the AE signal of lower amplitude, occurring over the whole load ranges, was considered to correspond to the formations of fibre breakage and matrix crack. The AE signal of higher amplitude, occurring in only the final load range, was considered to correspond to the formation of partial delamination.

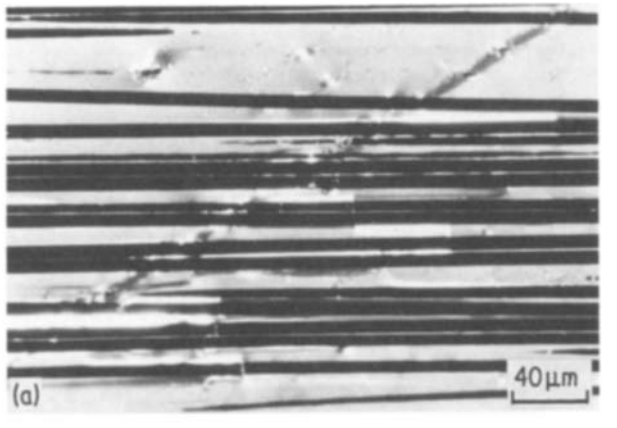

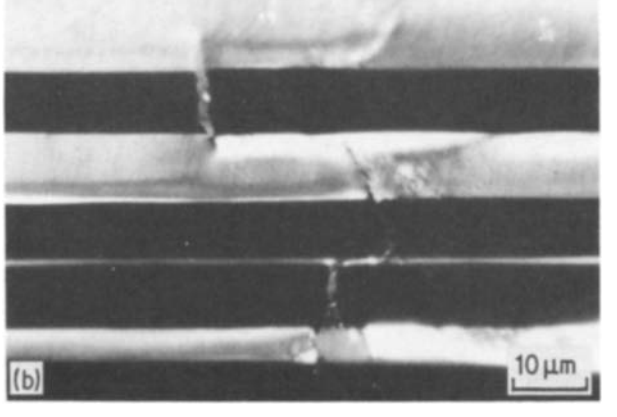

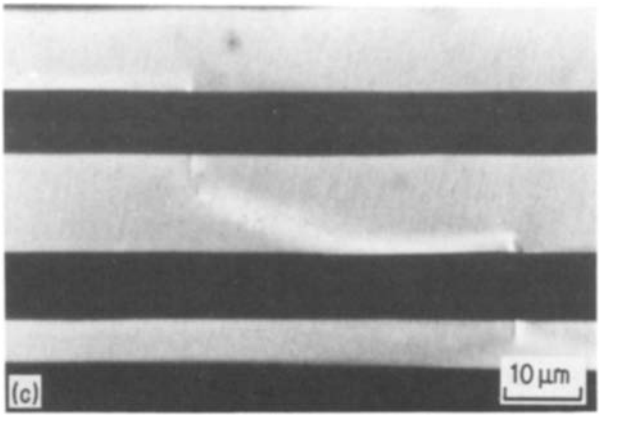

Figure 12 Polarized transmission optical micrographs of thin sections of composite with fibre breakage. The black line is carbon fibre and the rest is matrix. The brightened and darkened regions in the matrix indicate the region of plastic deformation. (a), (b) Plastic deformation starting from a fibre tip along the fibre sides. (c) Plastic deformation connecting fibre tips.

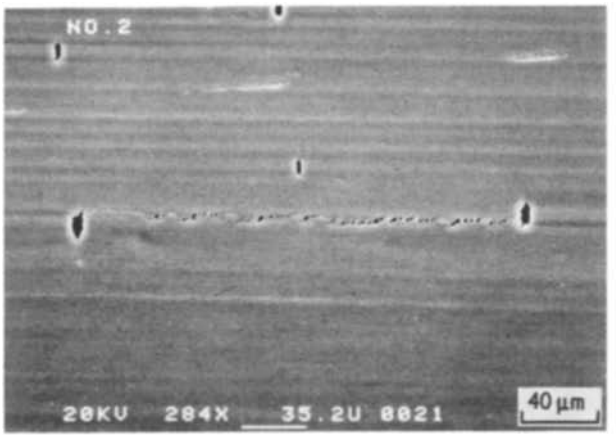

Figure 13 Matrix crack formation observed by SEM, showing a discontinuous crack propagation between broken fibre tips.

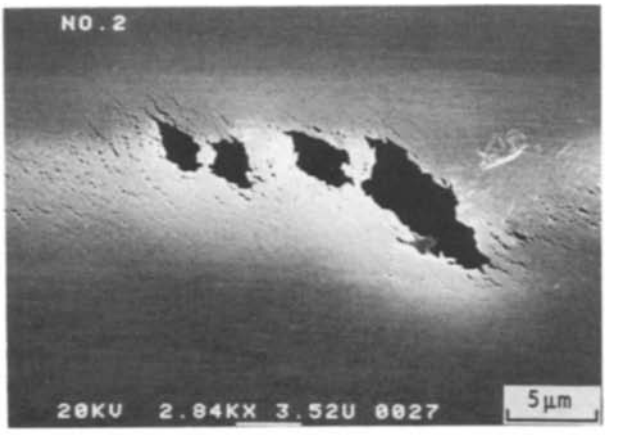

Figure 14 A magnified view of the matrix crack, showing sub-microcracks around it.

This supposition was supported by SEM observation that fibre breakage and matrix cracking were observed in all load ranges, and partial delamination was only observed just before failure.

Deformation and crack formation of the matrix were discussed in the light of the results of microscopic observation. The matrix used in this study showed a brittle fracture behaviour when it was subjected to a tension test. Its macroscopic fracture strain was about 3%, as listed in Table I. However, ductile deformation of the matrix was observed in the initial failure process of the composite. Fig. 12 shows the plastic deformation of the matrix accompanied by fibre breakage. The plastic deformation was formed by the shear stress concentration due to the fibre breakage. The matrix could be deformed in a ductile manner in a microscopic region near the broken fibre tip. The ductile deformation was considered to absorb the fracture energy of fibre. Therefore, matrix deformation accompanied by fibre breakage was considered to contribute to the fracture toughness of the composite.

Fig. 13 shows an interesting example of matrix crack formation obtained by *in situ* SEM observation. Matrix cracks were formed discontinuously in the region connecting broken fibre tips. Fig. 14 is a magnified view of a matrix crack, which shows the formation of sub-microcracks around the matrix crack. It was considered from these figures that sub-microcracks were formed in the region of plastic deformation and that some of them grew to voids, leading to discontinuous matrix cracks. Then, the deformation of the matrix in the failure process was described as follows. The matrix was deformed uniformly at the first stage. When a fibre was broken, the matrix around the fibre tip yielded due to the shear stress, and plastic deformation was formed along the fibre sides. As the shear stress was further increased, many sub-microcracks were formed in the plastic region and some of them grew to the matrix cracks. This mechanism was considered to be one reason why the matrix crack was formed discontinuously starting from the broken fibre tip.

5. Conclusions

The fracture mechanism of an unidirectional carbon fibre reinforced epoxy resin composite has been studied experimentally. The results obtained were as follows.

1. The detailed failure process of the composite was observed *in situ* by scanning electron microscopy. It was found that the failure progressed in the following order: fibre breakage, matrix cracking, partial delamination and final catastrophic crack propagation.

2. Matrix deformation accompanied by fibre breakage was examined by polarized optical microscopy and scanning electron microscopy. The matrix around the broken fibre tip was found to be deformed plastically due to the shear stress concentration. As the applied stress was further increased, sub-microcracks were formed in the plastic region and some of them grew to a matrix crack.

3. Acoustic emission monitoring was carried out at a three-point bending test. The AE data obtained were compared with the failure process obtained by *in situ* SEM observation at the same load range, and close correlation between AE amplitude and crack formation was observed. An AE signal of lower amplitude occurring in all load ranges was considered to correspond to the fibre breakage and matrix cracking. On the other hand, an AE signal of higher amplitude occurring just before failure was considered to correspond to the partial delamination.

The experimental procedure used in this study was considered to be useful for the study of the fracture mechanism of other composites.

References

1. C. ZWEBEN, *Amer. Inst. Aeronaut. Astronaut. J.* **6** (1968) 2325.
2. C. ZWEBEN and B. W. ROSEN, *J. Mech. Phys. Solids* **18** (1970) 189.
3. D. G. HARLOW and S. L. PHOENIX, *J. Comp. Mater.* **12** (1978) 195.
4. J. M. MAHISHI and D. F. ADAMS, *J. Mater. Sci.* **18** (1983) 447.
5. R. G. WHITE and H. TRETOUT, *Composites* **10** (1979) 101.
6. J. BECHT, H. J. SCHWALBE and J. EISENBLAETTER, *ibid.* **7** (1976) 245.
7. N. SATO, T. KURAUCHI, S. SATO and O. KAMIGAITO, *J. Mater. Sci. Lett.* **2** (1983) 188.
8. *Idem, J. Mater. Sci.* **19** (1984) 1145.

Received 18 February
and accepted 31 May 1985